ELSEVIER

Cement & Concrete Composites **17** (1995) 37–45

0958-9465/95/$9.50

Performance of Repaired Reinforced Concrete Slabs Under Static and Cyclic Loadings

P. Paramasivam, K. C. G. Ong, B. G. Ong & S. L. Lee

Department of Civil Engineering, National University of Singapore, Singapore

(Received 21 February 1994; accepted 11 October 1994)

Abstract

A total of 50 repaired and unrepaired reinforced concrete slab specimens were tested under static and cyclic loading conditions in this study. The specimens were of rectangular cross-section, 300 × 80 mm, and tested in flexure, simply-supported on a span of 600 mm under a line load at mid-span. Four types of specimens were tested. These include control specimens, which were unrepaired, and three other types of repaired specimens with cover reinstatement up to: the level of the reinforcing steel; mid-depth of the reinforcing steel; and full depth of the reinforcing steel, respectively. The performance of specimens statically-loaded to failure was monitored, while the deterioration of flexural rigidity of specimens subjected to cyclic loading was evaluated after being subjected to a predetermined number of cycles at various stress ranges. The results of experimental tests are summarized and discussed in this paper.

Keywords: Reinforced concrete slab, repair, deterioration, flexural rigidity, spalled cover, cyclic loading, durability.

INTRODUCTION

Nowadays, reinstatement of concrete cover in reinforced concrete slabs is not uncommon. This may be necessary due to an ingress of chloride ions and/or carbonation, particularly in structures exposed to extreme weather conditions. The work is of a specialized nature involving many operations and using specialized materials, frequently in unfavourable circumstances. Problems that are generally encountered in such repair work have been identified and possible solutions are presented in various specifications and guidelines. These include removal of unsound concrete, preparation of concrete bonding surfaces, cleaning and/or replacement of reinforcing steel, surface inspection and, finally, patch repair by prepacked cementitious mortar or any other suitable repair material, depending on the severity of the existing damage and exposure conditions.

As a result of the proliferation of many commercially available materials, there has been a fairly extensive use of such materials in the reinstatement of spalled cover for reinforced concrete slabs and beams. The apparent success with which such work has been carried out has demonstrated effectiveness under short term conditions. Performance in the long run, particularly under cyclic loading, remains a point of contention due mainly to a lack of adequate experimental evidence.

Therefore, the main objective of the study reported herein was to generate information on the performance and durability of repaired concrete slabs subjected to static and cyclic loadings. Since the thickness of concrete cover reinstatement may vary, it is important to study the effect of the position of the interface between concrete substrate and repair material with respect to the position of reinforcement, as this may significantly affect the performance and durability of the repaired structure under service loads, which are cyclical in nature.

TEST PROGRAMME

Test specimens

In this study, a total of 50 specimens were tested. All specimens were of rectangular cross-section, 300 × 80 mm. The specimens were 650 mm long provided with only longitudinal bar reinforcement. As can be seen in Fig. 1, three numbers of 8 mm diameter, smooth, mild steel bars, spaced

125 mm apart with a 20 mm clear cover, were used. Table 1 gives details of the test programme. The specimens were divided into four types, designated Type I, II, III and IV. These include control speciments, which were unrepaired, and three other types of repaired specimens with cover reinstatement up to: the level of the reinforcing steel; mid-depth of the reinforcing steel; and full depth of the reinforcing steel (Fig. 1).

Materials

Ordinary Portland cement, natural sand and 10 mm, maximum-size crushed granite were used in the proportions 1–2·11–2·68 with a water–cement ratio of 0·55. At least six 100 mm cubes, four 100 × 100 × 500 mm prisms and three 150 × 300 mm cylinders were cast, accompanying each batch of specimens, to determine the respective compressive strength, modulus of rupture and Young's modulus of elasticity of the concrete at the desired age. The properties of concrete at the age of 28 days are tabulated in Table 2.

The repair material used was a pre-packed, ready to use, shrinkage compensated, natural aggregate cementitious mortar. It was mixed to a trowellable consistency with the addition of water (3·2–3·4 litres for a 25 kg bag). Tests were conducted on 70 mm cubes, 100 × 100 × 500 mm prisms and 150 × 300 mm cylinders to determine the compressive strength, modulus of rupture and elasticity of the hardened mortar. The average compressive strength, modulus of rupture and modulus of elasticity values were found to be 57·8 N mm^{-2}, 4·88 N mm^{-2} and 25·5 kN mm^{-2}, respectively. Tensile tests on standard samples of the steel reinforcing bars gave an average yield strength of 332·2 N mm^{-2} and a Young's modulus of elasticity of 200 kN mm^{-2}.

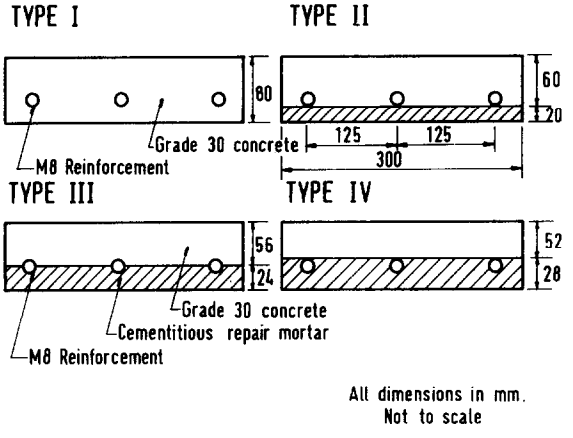

Fig. 1. Cross-section of test specimens.

Table 1. Distribution of specimens for testing

Specimen type	*Number of specimens tested*				*Total number of specimens*
	Static load	*Maximum value of applied cyclic load (% of ultimate static strength)*			
		25	*35*	*45*	
I	5	4	2	4	15
II	3	3	2	2	10
III	4	3	4	2	13
IV	4	2	4	2	12

Preparation of specimens

All the specimens were cast in wooden moulds and demoulded after 24 h. They were then moist-cured for three days, after which they were air-cured at ambient indoor laboratory conditions (27 ± 2°C and 80 ± 10% relative humidity) until they were repaired. In the cover reinstatement of the other three types of specimen, Types II–IV, proper preparation of the surface of the parent concrete to receive the repair mortar is extremely important. After 28 days of curing, the surfaces of the parent concrete were prepared by roughening using mechanical chipping. Then, reinforcing steel was cleaned and strain gauges were fixed on the reinforcement bars at mid-span before the 'spalled cover' was reinstated using the cementitious repair mortar to obtain specimens 80 mm

Table 2. Properties of concrete at 28 days

Specimen type	*Compressive strength (N mm^{-2})*		*Young's modulus of elasticity (kN mm^{-2})*		*Modulus of rupture (N mm^{-2})*	
	Mean	*Std dev.*	*Mean*	*Std dev.*	*Mean*	*Std dev.*
I	33·5	2·6	23·3	1·1	4·64	0·32
II	38·2	3·1	24·4	1·6	4·63	0·17
III	35·2	3·3	25·7	2·0	4·86	0·36
IV	35·9	4·2	26·7	0·9	4·92	0·34

thick. The application of this repair mortar was carried out with the concrete interface under saturated-surface dry conditions, as recommended by the manufacturer. All the repaired specimens were demoulded after 24 h and again moist-cured for three days before they were left to air-cure at ambient laboratory conditions until testing.

Test procedure

Static loading

Tests were conducted using a 500 kN, servo-controlled universal testing machine. The slab specimens were simply-supported on two line supports and loaded in flexure under a line load at mid-span on a span of 600 mm, as shown in Fig. 2. During each test, mid-span deflections and support deformations were monitored using LVDTs while electrical resistance strain gauges mounted on the reinforcing steel at mid-span were used to monitor strains in the reinforcement. The static load was applied in increments of 0·5 kN and after each increment, the formation and development of flexural cracks were marked and the widths of major cracks were measured using a hand-held microscope with an accuracy of ± 0·02 mm. Static loading was continued up to failure. The failure was governed by crushing of the compression zone concrete after the tensile reinforcing steel had yielded. The first crack load, ultimate strength, maximum crack width, total number of cracks and final failure mode were noted.

Cyclic loading

One specimen from each group was tested under a static load to obtain the basic flexural strength and, hence, to establish a guideline for the application of the cyclic loading. The remaining specimens in each group (at least two other specimens) were subjected to 100 000 cycles of cyclic loading. The load was cycled between a minimum of 1% and a maximum load level of either 25, 35 or 45% of the static ultimate flexural strength determined previously. The sinusoidal cyclic load was applied at a rate of 5 Hz. The rate chosen was in line with recommendations by the ACI Committee 215.[1] Previous investigations on fatigue of concrete, reported by the ACI Committee 215 have shown that the fatigue strength of concrete is not much affected by the rate of cyclic loading, for cycles within the frequency range 1–15 Hz, provided the maximum applied stress level is less than about 75% of its static strength.

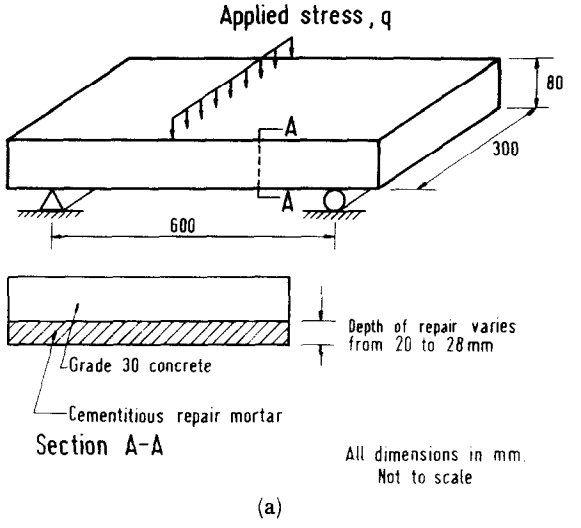

(a)

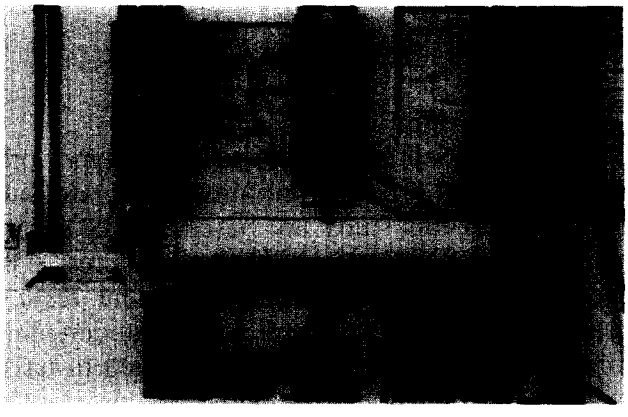

(b)

Fig. 2. Typical simply-supported reinforced concrete test specimen. (a) Test set-up; (b) slab ready for testing.

The deterioration of flexural rigidity of the specimens after being subjected to a predetermined number of cycles, viz. 5000, 10 000, 20 000, 50 000 and 100 000 cycles, were monitored. This was carried out by plotting the load vs mid-span deflection curve of specimens statically loaded up to 4 kN. This load was well below the virgin nominal first crack load of the specimen tested previously. Based on these load vs mid-span deflection curves, the experimental values of flexural rigidity of the specimen are computed from the slope of the straight line obtained. Assuming stress is proportional to strain before any cracking occurs, and that curvatures are small, the mid-span deflection of the specimens tested may be approximated by:

$$\delta = (k_1 P l^3)/EI \qquad (1)$$

where k_1, is a constant depending on type of loading and end restraints, P is the total load applied, l

is the span width and EI is the flexural rigidity. For the specimens tested, the theoretical value of $k_1 = 1/48$, thus:

$$(EI)_{exp} = (k_1 Pl^3)/\delta \quad (2)$$

which can be easily determined once P/δ (the slope obtained from the experimental load vs midspan deflection curve) is known. At least two specimens of each group were cast and tested in order to take into account the variation of the results due to the inherent variability of the materials used, fabrication, casting, repair and testing processes. A non-linear regression analysis was performed to compare deterioration of specimens under cyclic loading.

TEST RESULTS AND DISCUSSION

General behaviour

The predicted values of ultimate strength for both unrepaired and repaired reinforced concrete slab specimens in this study are based on BS 8110[2] and ACI-318.[3] Since the reinforced concrete slab specimens in the present experimental testing programme were designed to be under-reinforced, all reinforcing steel was assumed to have yielded at ultimate strength, as previously mentioned.

Cracks initiated at the soffit and propagated vertically upwards. The first crack load was observed to occur at 25–44% of the ultimate static strengths. Table 3 shows the average load at the first crack, the experimental ultimate static strength, values of first cracking and ultimate static strengths as ratios of their respective theoretical values from results of the static tests. For Type I specimens, both uncycled and cycled specimens exhibited higher ratios of experimental–theoretical values for both first crack and ultimate static strengths (average values of 0·79 and 1·25, respectively) compared to repaired specimens (0·59 and 1·07, respectively). However, no significant differences were observed in the above ratios for the three types of repaired specimens.

When tested under static loads it was observed that, as the load was increased, only a few vertical cracks were observed and all specimens recorded large crack openings at the onset of failure. Type I and II specimens failed in flexure. However, in the case of Type III and IV specimens, debonding at the concrete–repair mortar interface was noticed in a few specimens at failure. This is probably due to less efficient bonding at the concrete–steel and repair mortar–steel interfaces. Typical specimens at failure are shown in Fig. 3, while Figs 4–6 show the cracking patterns of both unrepaired and repaired specimens tested statically to failure at 0 cycles and after 100 000 cycles of cyclic loading. For uncycled specimens tested statically to failure (Fig. 4) it was observed that Type II specimens exhibited a similar cracking pattern as observed

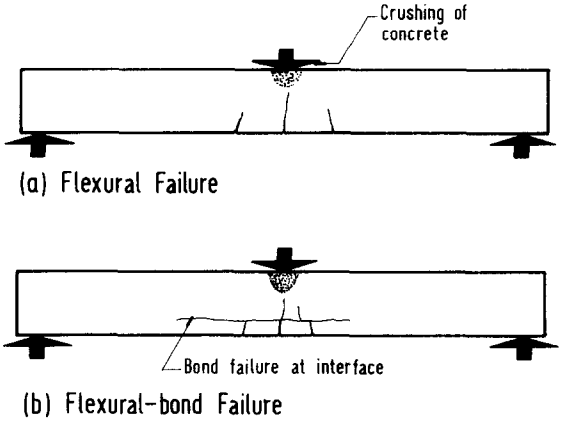

Fig. 3. Typical cracking patterns of specimens at failure.

Table 3. Results of static loading tests

Specimen type	*Average first crack strength (kN)*	$P_{cr,exp}/P_{cr,theo}$ *(average)*	*Average static ultimate strength (kN)*	$M_{u,exp}/M_{u,theo}$ *(average)*	*Failure mode*
I	8·16	0·79	18·49	1·25	Flexural failure
II	7·01	0·72	17·25	0·98	Flexural failure
III	4·36	0·41	17·39	1·02	Flexural failure with total debonding at concrete–mortar interface in a few specimens
IV	6·56	0·62	19·27	1·16	Flexural failure with debonding at concrete–mortar interface in a few specimens

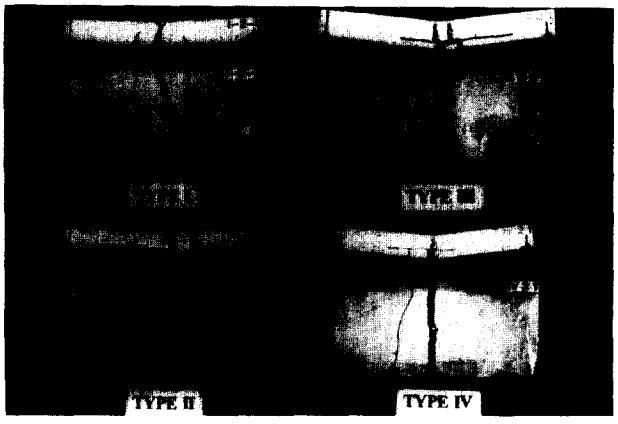

Fig. 4. Crack patterns of all four types of specimens tested under static load.

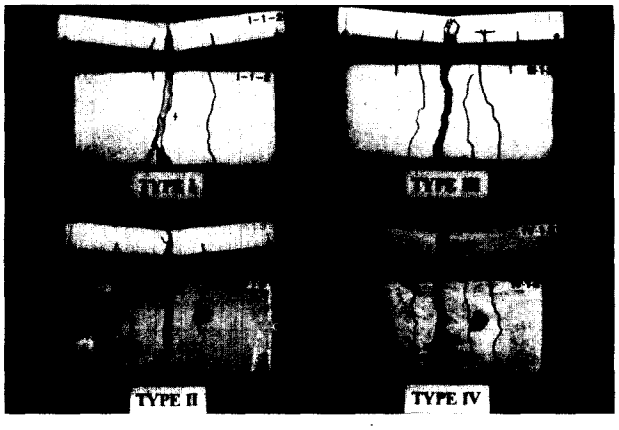

Fig. 5. Crack patterns of all four types of specimens tested statically to failure after 100000 cycles of applied stress at 25% of ultimate static strength.

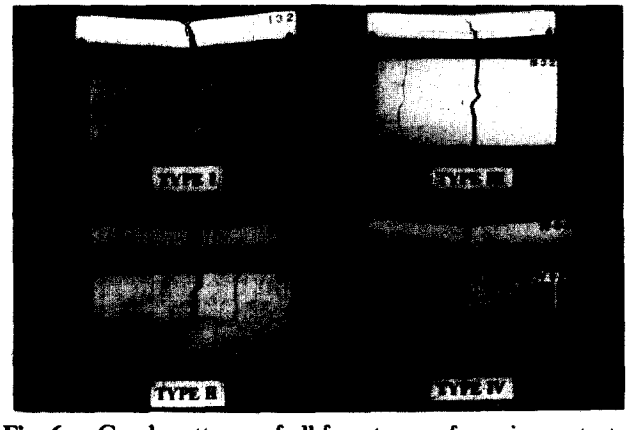

Fig. 6. Crack patterns of all four types of specimens tested statically to failure after 100000 cycles of applied stress at 45% of ultimate static strength.

on Type I specimens, whereas Type III and IV specimens exhibit flexural cracking with debonding between concrete and repair mortar interfaces.

In Figs 5 and 6, it may be observed that after 100000 cycles as the maximum applied load was increased from 25 to 45%, lesser numbers of flexural cracks were observed at failure. It may also be seen that some Type III and Type IV specimens failed in the flexural bond mode rather than flexural failure.

Effects of applied stress

In the present study, the maximum level of applied cyclic loading, q_{max}, was fixed at 25, 35 and 45% of the respective ultimate static strengths, as mentioned previously. The results of cyclic tests obtained are tabulated in Table 4. Figure 7 shows a plot of normalized flexural rigidity (ratio of flexural rigidity after n cycles–virgin flexural rigidity, i.e. EI_n/EI_0) vs number of cycles of cyclic loading for Type I specimens tested with maximum cyclic loads of 25, 35 and 45% of the respective experimental ultimate static strengths. As the applied maximum cyclic load was increased from 25 to 35 and 45% of the respective ultimate static strength, greater degradation (increasing from 3 to 19 and 24%, respectively) in normalized flexural rigidity was observed after 5000 cycles. The respective values became 4, 26 and 32% after 100000 cycles of loading. This was probably due to progressive deterioration of the bond between the concrete and the reinforcing steel. This may be attributed to higher creep strain or deformation of compression-zone concrete and reduction in stiffness contribution of tension-zone concrete due to fatigue–tensile cracking.[4]

Type II specimens behaved very similar to Type I specimens at lower levels of applied cyclic loading, i.e. 25–35%, which was well below the cracking load of the specimens (Fig. 8). Type IV specimens on the other hand showed a higher decrease in flexural rigidity compared with Type I and II specimens after cyclic loading. Debonding was observed at the concrete–repair mortar interface at failure in a few specimens. In the case of Type III specimens a severe drop in flexural rigidity (30–65%) after only 5000 cycles was observed and total debonding at the concrete–repair mortar interface occurred in a few specimens at failure. Detailed information on the degree of deterioration of flexural rigidity for repaired and unrepaired reinforced concrete slab specimens subjected to cyclic loading can be obtained from the relationships of normalized flexural rigidity, $r(EI_{n'}/EI_{0'})$, and number of constant amplitude cycles, n, as tabulated in Table 5.

Table 4. Results of cyclic loading tests

Specimen type	Maximum applied cyclic load q_{max} (% of ultimate static strength)	Average residual ultimate strength (kN)	$M_{u,exp}/M_{u,theo}$ (average)	$(EI_0 - EI_n)/EI_0$ (%)		Failure mode†
				After 5000 cycles	After 100000 cycles	
I	25	17·47	1·24	3·1	4·2	Flexural failure
	35	18·54	1·23	19·4	26·2	
	45	19·65	1·27	23·8	32·1	
II	25	17·14	1·03	1·8	2·4	Flexural failure
	35	17·89	1·05	15·8	21·4	
	45	18·10	1·07	42·8	57·9	
III	25	17·23	1·03	30·2	40·8	Flexural failure with total debonding at concrete-mortar interface in a few specimens
	35	17·78	1·06	33·8	45·7	
	45	16·96	1·01	64·6	87·3	
IV	25	18·85	1·15	15·9	21·5	Flexural failure with debonding at concrete-mortar interface in a few specimens
	35	19·49	1·16	32·0	43·3	
	45	18·83	1·14	38·2	51·7	

†Tested statically to failure after 100 000 cycles.

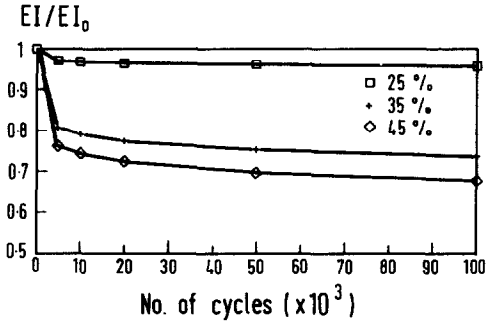

Fig. 7. Normalized flexural rigidity vs number of cycles for Type I specimens at various load levels.

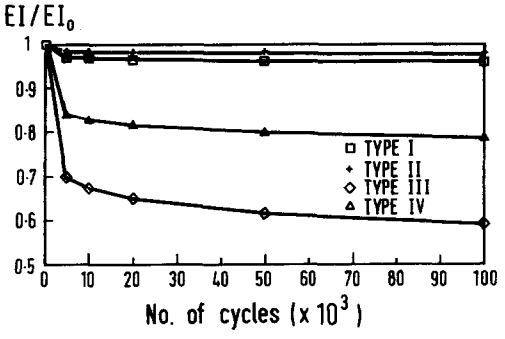

Fig. 8. Normalized flexural rigidity vs number of cycles for various types of specimens cycled at 25% of ultimate static strength.

For the three types of repaired specimens tested, it was observed that the higher the applied cyclic load level, the more significant was the decrease in flexural rigidity. It was reported by

Table 5. Relationship between normalized flexural rigidity, $r(EI_n/EI_0)$, and number of constant amplitude cycles, n

Specimen type	Maximum applied cyclic load, q_{max} (% of ultimate static strength)	$r = EI_n/EI_0$
I	25	$r = 1{\cdot}00 - 0{\cdot}0037 \ln n$
	35	$r = 1{\cdot}00 - 0{\cdot}0228 \ln n$
	45	$r = 1{\cdot}00 - 0{\cdot}0279 \ln n$
II	25	$r = 1{\cdot}00 - 0{\cdot}0021 \ln n$
	35	$r = 1{\cdot}00 - 0{\cdot}0186 \ln n$
	45	$r = 1{\cdot}00 - 0{\cdot}0503 \ln n$
III	25	$r = 1{\cdot}00 - 0{\cdot}0354 \ln n$
	35	$r = 1{\cdot}00 - 0{\cdot}0397 \ln n$
	45	$r = 1{\cdot}00 - 0{\cdot}0758 \ln n$
IV	25	$r = 1{\cdot}00 - 0{\cdot}0187 \ln n$
	35	$r = 1{\cdot}00 - 0{\cdot}0376 \ln n$
	45	$r = 1{\cdot}00 - 0{\cdot}0499 \ln n$

Balaguru *et al.*[5] for the low-cycle fatigue loading test that cyclic creep strain in the reinforcing bars was not significant, thus, it may be assumed that the reinforcing bars were cyclically stable at these working load levels. Again, no significant difference (less than 10%) was observed when comparing ultimate static strength of uncycled specimens and residual static strength of those specimens cycled up to 100 000 times.

Effects of depth of concrete cover reinstatement

The minimum, maximum and average values of depth of repair-material were measured after the specimens were tested to failure at the end of

cyclic loading tests. The mean and standard deviation of these values are as follows:

Type II: mean, 23·0 mm; standard deviation 1·9 mm.
Type III: mean, 25·4 mm; standard deviation, 1·4 mm.
Type IV: mean, 28·3 mm; standard deviation, 1·5 mm.

On average, experimental results showed that Type II specimens exhibited a good cracking strength of 7·01 kN (about 40% of its ultimate static strength) compared to unrepaired Type I specimens, which recorded an average value of 8·16 kN (about 44%). On the other hand, Type IV specimens performed slightly better in terms of cracking strength (6·56 kN, i.e. about 34% of its ultimate strength) when compared to Type III specimens, which showed the lowest average of 4·36 kN (25% of its ultimate static strength). However, there were no significant differences in the experimental ultimate static strengths of both unrepaired and repaired specimens.

As mentioned earlier, at lower levels of applied cyclic loading, all specimens failed in the flexural mode except for some Type III specimens, where cover reinstatement resulted in the coincidence of the interface between concrete and cementitious repair mortar with a horizontal plane through the centre of the reinforcing bars. Flexural failure (Fig. 3(a)) was initiated by widening of one of the vertical cracks as the midspan deflection was increased. The final failure was caused by crushing of concrete and yielding of reinforcing steel. However, some Type III specimens failed in the flexural-bond mode, with total debonding at the interface between concrete substrate and repair mortar, as shown in Fig. 6. Such debonding may be caused by the difference in bond stresses at the concrete–steel and repair mortar–steel interfaces, since the steel bars are in contact with both concrete and repair mortar. Where debonding occurred, a crack was observed to propagate horizontally along the concrete repair material interface towards the support. Nevertheless, the specimens tested attained their full flexural capacity with crushing of concrete and yielding of the longitudinal steel reinforcement at failure. It was observed that these specimens also recorded the lowest first crack load, as mentioned earlier.

In contrast, results showed that Type II and IV specimens exhibited good composite action between concrete and repair mortar. This may be due to the larger bonding surfaces between reinforcing steel and either concrete or cementitious repair mortar in Type II (more than 80% between steel and concrete) and Type IV specimens (almost 100% between steel and repair mortar). With the larger bonding surface between steel and concrete alone or steel and repair mortar alone, lower degradation in flexural rigidity was obtained, thus improving the performance and durability of the repaired specimens. However, when cycled at higher levels of applied cyclic loading (35–45%), some debonding between concrete and repair mortar was observed in a few Type IV specimens at failure (Fig. 6).

Silfwerbrand[6] investigated the repair of reinforced concrete beams using shotcrete and recommended that the bonding interfaces of repair should not coincide with a horizontal plane through the centre of the reinforcement used. Therefore, based on results obtained in the present study, the performance of Type III specimens, where the concrete–repair mortar interface coincides with a horizontal plane through the centre of reinforcing bars, was not satisfactory.

Figures 8 and 9 show a typical plot of degradation of flexural rigidity for all four types of specimen tested with maximum cyclic loads of 25 and 45% of their respective experimental ultimate static strengths. Type III specimens consistently exhibited the largest degradation in flexural rigidity.

If the effects of level of cyclic loading are ignored, a simplistic model to assess the performance of the four types of specimen may be of the form:

$$r = a - b \ln(n) \tag{3}$$

where: r is the normalized flexural rigidity, i.e. the ratio of flexural rigidity (after n cycles)–virgin flexural rigidity (EI_n/EI_0); and n is the number of cycles of constant amplitude cyclic loading.

This relation is demonstrated in Fig. 10, where a consistent trend was noticed for all four types of specimens, irrespective of the level of cyclic loading. Values of a and b are empirical constants which were evaluated by conducting a regression analysis of the experimental data. The constant a was evaluated to be unity for all four types of specimen and b was 0·00187, 0·00206, 0·0453 and 0·0377 for specimens I–IV, respectively. The total decrease in flexural rigidity after 100 000 cycles of cyclic loading, irrespective of the applied level of cyclic loading, for Type I–IV specimens, was 21·5, 23·7, 52·2 and 43·4%, respectively.

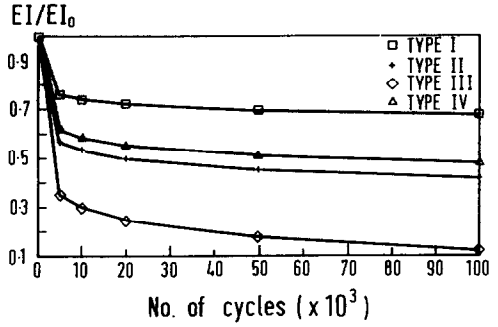

Fig. 9. Normalized flexural rigidity vs number of cycles for various types of specimens cycled at 45% of ultimate static strength.

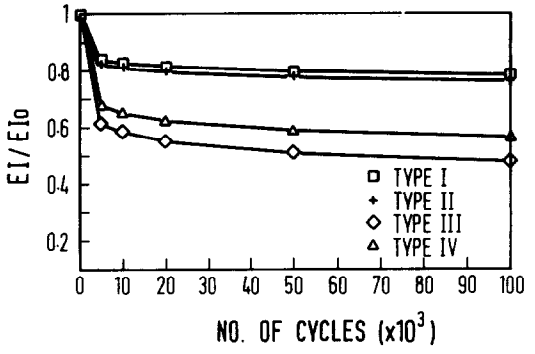

Fig. 10. Normalized flexural rigidity vs number of cycles for various types of specimens irrespective of applied stresses.

Performance of repaired reinforced concrete slabs

Based on the relationships shown in Table 5 and assuming r to be normally distributed, the residual flexural rigidity of Type I specimens after 100 000 cycles will lie between the intervals shown in Table 6, with a 90% confidence level. The performance of Type II–IV specimens under the same loading conditions may be compared with the values shown in Table 6. Using the residual flexural rigidity of Type I specimens after 100 000 cycles of cyclic loading as a basis for comparison, Table 7 shows that Type II specimens outperformed Type I specimens when subjected to cyclic loads of 25 and 35% of the experimental static strength. This is indicated by the fact that the number of cycles to achieve the same level of residual flexural rigidity after cyclic loading exceeds 100 000 cycles (by interpolation). When the applied stress level was increased to 45%, only 3150 cycles are needed to achieve the same level of residual flexural rigidity as that for the Type I specimen after 100 000 cycles.

In contrast, Type III specimens recorded the least number of cycles to achieve the respective values of residual flexural rigidity of Type I specimens for all three levels of applied cyclic loading. In the case of Type IV specimens, a performance very similar to Type III specimens was seen at lower applied stresses. However, when subjected to cyclic loads of 45% of ultimate static strength, Type IV specimens outperformed Type II specimens in terms of residual flexural rigidity. This can be seen from the number of equivalent cycles to achieve the same residual flexural rigidity as that of Type I specimens. However, more experimental results are required to confirm the trend of these results.

Table 6. Residual flexural rigidity for Type I specimens after 100 000 cycles of cyclic loading at various load levels

Maximum applied cyclic load, q_{max} (% of ultimate static strength)	*Interval of residual flexural rigidity with 90% confidence level*
25	0·9249; 0·9699
35	0·6634; 0·7292
45	0·5268; 0·6630

Table 7. Performance of Type II–IV specimens with respect to Type I specimens

Specimen type	*Number of equivalent cycles to achieve same residual flexural rigidity of Type I specimens cycled up to 100 000 cycles at various load levels (% of ultimate static strength)*		
	25	*35*	*45*
II	> 100 000	> 100 000	3150
III	< 10	2100	210
IV	20	3220	8290

CONCLUSIONS

(1) For unrepaired, Type I specimens, higher degradation in normalized flexural rigidity was observed due to higher values of applied cyclic loading. However, the experimental results showed no significant loss in residual ultimate static strengths after 100 000 cycles of loading with a maximum cyclic load of up to 45% of the experimental static strength.

(2) For all the three types of repaired specimen tested, namely Types II–IV, it was observed that the higher the applied cyclic load level, the more significant was the decrease in flexural rigidity after cyclic loading.

(3) The behaviour of Type II specimens is similar to unrepaired specimens at a lower stress level. Both types failed in flexure under static and after cyclic load tests. Specimens tested with maximum cyclic load levels up to 45% of the ultimate static strength exhibited good fatigue resistance in terms of residual ultimate static strengths.

(4) Type IV specimens showed a higher decrease in flexural rigidity than Type I and II specimens after cyclic loading. When cycled at higher levels of applied cyclic loading (35 and 45%) some debonding between concrete and repair mortar was observed in a few specimens.

(5) The interface between concrete and cementitious repair mortar should not coincide with the horizontal plane through the centre of the reinforcing bars (Type III specimens). Results showed total debonding at the concrete–repair mortar interface under both static and cyclic loading tests in a few specimens. They also show significantly larger degradation of flexural rigidity after only 5000 cycles and at the end of cyclic loading tests.

ACKNOWLEDGEMENT

The research reported in this paper was made possible through the financial support of the National Science and Technology Board (NSTB) under the Research and Development Assistance Scheme (RDAS) Grant ST/88/04. This support is gratefully acknowledged.

REFERENCES

1. ACI Committee 215, Considerations for design of concrete structures subjected to fatigue loading. *ACI J.*, **71** (3)(1974) 97–120.
2. BS 8110: Part 1, *Structural Use of Concrete*. British Standards Institution, London, 1985.
3. ACI-318, *Building Code Requirements for Reinforced Concrete*. American Concrete Institute, Detroit, Michigan, 1983.
4. Balaguru, P. & Shah, S. P., A method of predicting crack widths and deflections for fatigue loading. In *Fatigue of Concrete Structures*, ed. S. P. Shah, ACI Publication SP-75, Detroit, pp. 153–75, 1982.
5. Balaguru, P., Naaman, A. E. & Shah, S. P., *Ferrocement in Bending, Part II: Fatigue Analysis*. Report No. 77-1, Dept of Materials Engineering, University of Illinois, Chicago, Oct. 1977.
6. Silfwerbrand, J., Concrete repair with shotcrete. *TABSE Symposium*, Lisbon, pp. 785–90, 1989.